Transcriptional crosstalk varies between regulatory strategies

Rok Grah(1) and Tamar Friedlander(2)

(1) Institute of Science and Technology Austria, Am Campus 1, A-3400 Klosterneuburg, Austria

(2) The Robert H. Smith Institute of Plant Sciences and Genetics in Agriculture

Faculty of Agriculture, Hebrew University of Jerusalem,

P.O. Box 12 Rehovot 7610001, Israel

March 19, 2019

Abstract

Genes differ in the frequency at which they are expressed and in the form of regulation used to control their activity. In particular, positive or negative regulation can lead to activation of a gene in response to an external signal. Previous works proposed that the form of regulation of a gene correlates with its frequency of usage: positive regulation when the gene is frequently expressed and negative regulation when infrequently expressed. Such network design means that, in the absence of their regulators, the genes are found in their least required activity state, hence regulatory intervention is often necessary. Due to the multitude of genes and regulators, spurious binding and unbinding events, called "crosstalk", could occur. To determine how the form of regulation affects the global crosstalk in the network, we used a mathematical model that includes multiple regulators and multiple target genes. We found that crosstalk usually increases with the availability of regulators. Our analysis showed that excess use of regulation entailed by the formerly suggested network design caused high crosstalk levels in a large part of the parameter space. We therefore considered the opposite 'idle' design, where the default unregulated state of genes is their frequently required activity state. We found, that 'idle' design minimized the use of regulation and thus minimized crosstalk. In addition, we estimated global crosstalk of *S. cerevisiae* using transcription factors binding data. We demonstrated that even partial network data could suffice to estimate its global crosstalk, suggesting its applicability to additional organisms. We found that *S. cerevisiae* estimated crosstalk is lower than that of a random network, suggesting that natural selection reduces crosstalk. In summary, our study highlights the impact of a new type of protein production cost which is typically overlooked: that of regulatory interference caused by the presence of excess regulators in the cell. It demonstrates the importance of whole-network descriptions, which could show effects missed by single-gene models.

Author Summary

Genes differ in the frequency at which they are expressed and in the form of regulation used to control their activity. The basic level of regulation is mediated by different types of DNA-binding proteins, where each type regulates particular gene(s). We distinguish between two basic forms of regulation: positive – if a gene is activated by the binding of its regulatory protein, and negative – if it is active unless bound by its regulatory protein. Due to the multitude of genes and regulators, spurious binding and unbinding events, called "crosstalk", could occur. How does the form of regulation, positive or negative, affect the extent of regulatory crosstalk? To address this question, we used a mathematical model integrating many genes and many regulators. As intuition suggests, we found that in most of the parameter space, crosstalk increased with the availability of regulators. We propose, that crosstalk is usually reduced when networks are designed such that minimal regulation is needed, which we call the 'idle' design. In other words: a frequently needed gene will use negative regulation and conversely, a scarcely needed gene will employ positive regulation. In both cases, the requirement for the regulators is minimized. In addition, we demonstrate how crosstalk can be calculated from available datasets and discuss the technical challenges in such calculation, specifically data incompleteness.

Introduction

Gene regulatory networks can employ different architectures that seemingly realize the same input-output relation. There is a basic dichotomy of gene regulation into positive and negative control. A gene controlled by positive regulation is, by default, not expressed and requires binding of an activator to its operator to induce it. In contrast, a gene controlled by negative regulation, is expressed by default, unless a repressor binds its operator and attenuates its activity. While a gene can be regulated using either mode, researchers have pondered whether additional considerations could favor the choice of one mechanism over the other, or whether this choice is merely a coincidence ("evolutionary accident"). Throughout the years, this question was addressed using different approaches. The seminal work of Michael Savageau [1, 2, 3] proposed the so-called "Savageau demand rule", namely, that genes encoding frequently needed products ("high-demand") are often regulated by activators. Conversely, genes whose products are only needed sporadically ("low-demand"), tend to be regulated by repressors. This finding was based on a survey of a limited set of bacterial genes known at that time. Savageau used an evolutionary argument to explain this finding, later called the "use-it-or lose-it" principle [4]. He considered mutations and selection affecting the regulatory construct, and argued that the intensity of selection depends on the extent to which it is used. If the regulatory construct is infrequently used (as in activator regulating a low-demand or a repressor regulating a high-demand gene), selection is weak and it is unlikely to survive. In contrast, if it is frequently used (activator regulating a high-demand or repressor regulating a low-demand gene), selection is stronger and this form of regulation is more likely to survive [5]. A later evolutionary analysis mathematically formulated the problem as selection in an alternating environment and found the exact conditions under which the Savageau demand rule is expected to hold [4].

An alternative reasoning for the observed correlation between a gene's demand and its form of regulation was later proposed using a biophysical, rather than an evolutionary argument [6, 7]. There, it was suggested, that the Savageau demand rule minimizes transcriptional crosstalk, because the regulatory binding sites are mostly occupied by their cognate regulators. When occupied, these sites are protected from random binding of for-

eign proteins that could interfere with the gene's regulatory state. A possible critique of this reasoning is the extravagant use of regulators it entails: both high- and low-demand genes require regulators most of the time, which would place heavy demands on protein expression systems, associated with reduced organismal fitness [8, 9, 10].

Recently, a comprehensive survey of regulatory topologies in *E. coli* and *B. subtilis*, found many exceptions to the Savageau demand rule. The authors proposed that evolutionary processes randomly pick a regulatory topology out of the many possible ones meeting the organism physiological constraints [11].

While the above-mentioned studies examined the significance of regulatory architectures from different perspectives, they all concentrated on a single gene with a single regulator (with potential external interference). They did not consider the additional regulatory interactions between each regulator and all other genes at play. While each interaction alone could be weak, an enormous number of such interactions occur and their total effect is significant [12, 13]. Here, we focus on the effects of transcriptional crosstalk and how it might dictate the choice between different regulatory topologies. We specifically refer to *global crosstalk*, which simultaneously accounts for crosstalk in all genes, rather than the single-gene crosstalk considered earlier.

We use a mathematical global crosstalk model [13], which was built upon the well-established thermodynamic model of gene regulation to calculate transcription factor (TF)-DNA interactions [14, 15, 16, 17, 18, 19, 20]. We have previously shown that while crosstalk affecting a particular gene can be reduced by different means, it always comes at the cost of elevating crosstalk in other genes. In contrast, the *global* crosstalk cannot be reduced below a certain threshold. Here, we analyze global crosstalk levels under different regulatory strategies: either positive or negative regulation. We compare two extreme designs: a "busy" one that implements the Savageau demand rule, in which a high (low)-demand gene is always regulated by an activator (repressor) and an opposite "idle" design, in which a high (low)-demand gene is always regulated by a repressor (activator). We find that the "busy" design maximizes regulator usage, whereas the "idle" one minimizes it. Since global crosstalk depends on the abundance of regulatory proteins in the cellular environment, we conclude that under most biologically plausible parameter values, the "idle" design should

yield lower *global* transcriptional crosstalk.

This paper begins with the introduction of a general symmetric model for the analysis of transcriptional crosstalk in a many-TFs-many-genes setting, with combination of positive and negative regulation. We show that global crosstalk levels directly depend on the fraction of TFs in use and only indirectly on the choice of activation or repression as the form of regulation. We then analyze TF usage and crosstalk levels of the two extreme designs, i.e., "busy" and "idle" and then construct numerical simulations of a more general asymmetric gene usage model, that are in agreement with the analytical result. Lastly, we discuss the challenges in crosstalk calculation for real gene regulatory networks, in particular, the possible effect of data incompleteness, and show an example using *S. cerevisiae* TF data.

Results

A model of gene regulation using a combination of activators and repressors

We consider a cell that has a total of M genes, each of which is transcriptionally regulated to be either active or inactive. We assume that each gene is regulated by a single unique TF species - its cognate one. Each gene has a short DNA binding site to which its cognate TF binds. A fraction $0 \leqslant p \leqslant 1$ of the genes is regulated by activators and the remaining $1-p$ fraction of genes is regulated by repressors. When no activator is bound, activator-regulated genes are inactive (or active at a low basal level) and only become active once an activator TF binds their binding site. In contrast, repressor-regulated genes are active, unless a repressor TF binds their binding site and inhibits their activity (Fig 1A). We assume that different environmental conditions require the activity of different subsets of the M genes. We assume however that all these subsets include the same proportion of genes $0 \leqslant q \leqslant 1$ that is needed to be active. The remaining $1-q$ proportion should be inactive. These activity states are regulated by the binding and unbinding of the TFs specialized for these genes. We assume that only a subset of TFs necessary to maintain the desired regulatory pattern, are available to bind and regulate these genes. However, TFs often have limited specificity to their DNA targets and can occasionally bind slightly different sequences, albeit

with lower probability [21, 22, 23, 24, 25].

We define 'crosstalk', which potentially leads to an undesired regulatory outcome, as cases in which a binding site that should be bound by a specific TF is instead bound by a non-cognate one or remains unbound (x_{bound}), or in which a binding site that should have been unbound is occupied (x_{unbound}) - see Fig 1C. To quantitate the probability of these events, we use the thermodynamic model of gene regulation [14, 15, 16, 17]. A mathematical model for crosstalk for the special case in which all TFs are activators ($p = 0$) was derived and analyzed in a previous work [13]. Here, we analyze a more general model with a combination of activators and repressors. The reader can find the details of both models in the SI of this paper.

Both activity and inactivity of genes can be attained by means of either activator or repressor regulation. Accordingly, our model distinguishes between four sets of genes (see Table below and Fig 1B):

Activity	Regulated by	Proportion of genes using this regulatory strategy
active	activator	a, where $a \leqslant q, p$
active	repressor	$q - a$
inactive	activator	$p - a$
inactive	repressor	$(1 - p) - q + a$

The probability that a particular gene i is in the x_{bound} or x_{unbound} crosstalk states, depends on the copy number of competing non-cognate TFs, C_j, $j \neq i$ and on the number of mismatches, d_{ij}, between each competing TF j and the regulatory binding site of gene i, where we assume equal energetic contributions of all positions in the binding site. Consequently, the similarity between binding sites regulated by distinct TFs is a major determinant of crosstalk. We introduce an average measure of similarity between binding site i and all other binding sites $j \neq i$ [13]:

$$S_i \equiv \langle e^{-\epsilon d_{ij}} \rangle_{P(d)} = \frac{1}{C} \sum_{j \neq i} C_j e^{-\epsilon d_{ij}} = \frac{1}{T} \sum_{j \neq i} e^{-\epsilon d_{ij}}. \tag{1}$$

As only a subset of the genes is regulated, the summation of only the corresponding

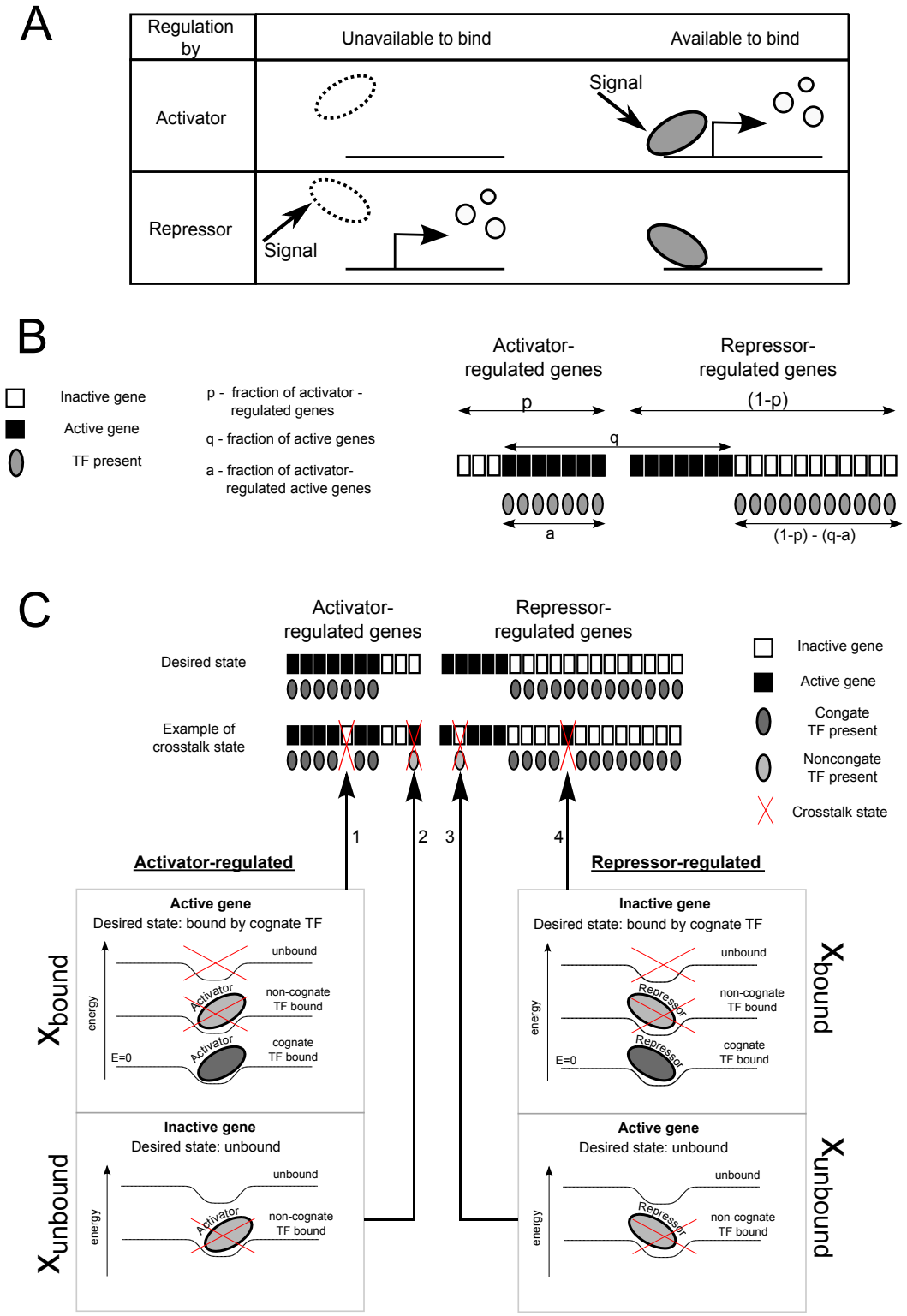

Figure 1: (Continued on the following page.)

Figure 1: **Gene regulation can employ different combinations of activators and repressors to implement the same gene expression pattern.** **(A)** A signal can cause gene activation by either positive (first row) or negative (second row) control. **(B)** We consider a total of M genes in a cell, of which fraction $0 \leqslant p \leqslant 1$ is regulated by activators, and the remaining $1-p$ is regulated by repressors. Assume that only fraction $q < 1$ of these genes should be active under certain conditions (black squares), while the remaining genes should be inactive (white squares). In general, $a \leqslant q, p$ of this q proportion is activator-regulated and $q-a$ is repressor-regulated. Here, we illustrate all four cases of active/inactive genes regulated by activator/repressor and define all the variables. Gray ellipses represent TFs (of either type) required to maintain the regulatory state of the genes. **(C)** Different genes are regulated by different TF species, where TF specificity is determined by short regulatory DNA sequences (binding sites) adjacent to the gene. Each such binding site can be at different levels of energy depending on its TF occupancy. It is in the lowest $E = 0$ (most favorable) level when bound by its cognate TF; it can be in a variety of higher energy levels if a non-cognate TF binds or if the site remains unoccupied (lower panel). The upper panel shows the crosstalk-free 'desired state' (first row), where each TF binds its cognate target. Below (second row), four different possibilities in which binding of a TF to non-cognate binding sites or failure to bind lead to crosstalk. An activator-regulated gene should ideally be regulated by its cognate activator (right-inclined ellipse), in order to become active. If this cognate TF fails to bind when the gene should be active (1), or if another TF binds when the gene should remain inactive (2), we consider this as crosstalk. For a repressor-regulated gene, crosstalk states occur when a non-cognate repressor binds when the gene should be active (3), or if the cognate repressor fails to bind when the gene should be inactive (4). We present cognate TFs by dark gray and non-cognate ones by light gray. Activators are represented by right-inclining and repressors by left-inclining ellipses. Crosstalk states are marked by red crosses.

subset of TFs available to bind is taken. S_i is defined as the average of the Boltzmann factors, $e^{-\epsilon d_{ij}}$, taken over the distribution of mismatch values $P(d)$ between binding sites i and j, $\forall j$. In the last equality in Eq. (1), we assume that all available TFs are found in equal concentrations $C_j = C/T, \forall j$, where C is the total TF concentration and T is the number of distinct TF species available. We found that allowing different concentrations for activators and repressors does not reduce crosstalk below this equal concentration scheme (SI). We also assume full symmetry between binding sites i, such that $S_i = S \ \forall i$. A theoretical analysis of a more general case with unequal S_i values can be found in SI. The value of S can be either estimated using binding site data (see below) or analytically calculated under different assumptions on the pairwise mismatch distribution $P(d)$. In the following, we use rescaled variables: $s = S \cdot M$ for rescaled similarity between binding sites, the fraction of available TFs ($t = T/M$) and the rescaled total TF concentration ($c = C/M$).

We distinguish crosstalk states of genes whose desired state of activity requires unoc-

cupied binding sites (x_{unbound}), and those requiring occupation by a cognate regulator (x_{bound}). x_{unbound} crosstalk includes the cases of an activator-regulated gene that should remain inactive as well as that of a repressor-regulated gene that should be active, both requiring an unoccupied binding site. For these genes, the cognate TF is not available to bind and any binding event by another (non-cognate) regulator is considered crosstalk. x_{bound} crosstalk includes both an activator-regulated gene that should be active and a repressor-regulated one that should be inactive. For these, crosstalk states occur either if the binding site remains unbound or if it is occupied by a non-cognate regulator, in which case, the regulatory state is not guaranteed. For illustration of all possible crosstalk states, see Fig 1C. Using equilibrium statistical mechanics, these crosstalk probabilities for a single gene i are [15, 16, 13]:

$$x_{\text{bound}} = \frac{e^{-E_a} + \sum_{j\neq i} C_j e^{-\epsilon d_{i,j}}}{C_i + e^{-E_a} + \sum_{j\neq i} C_j e^{-\epsilon d_{i,j}}} = \frac{e^{-E_a} + cs}{c/t + e^{-E_a} + cs} \tag{2a}$$

$$x_{\text{unbound}} = \frac{\sum_{j\neq i} C_j e^{-\epsilon d_{i,j}}}{e^{-E_a} + \sum_{j\neq i} C_j e^{-\epsilon d_{i,j}}} = \frac{cs}{e^{-E_a} + cs}. \tag{2b}$$

E_a is the energy difference between cognate bound and unbound states. The expression $\sum_{j\neq i} C_j e^{-\epsilon d_{ij}}$ captures the sum of all interactions of binding site i with foreign regulators.

Global crosstalk depends on the use of regulators

We define the global crosstalk, X, of a cell as the average fraction of genes found in any of the crosstalk states. For a given value of a, we average over different choices of a active genes out of the p activator-regulated and over different choices of $q-a$ out of the $(1-p)$ repressor-regulated proportions. The weighted sum over these four types of contributions provides the average total crosstalk, X, of the whole system:

$$\begin{aligned} X &= \overbrace{a \cdot x_{\text{bound}} + (p-a) \cdot x_{\text{unbound}}}^{\substack{\text{Contribution of}\\ \text{activator-regulated genes}}} + \overbrace{(q-a) \cdot x_{\text{unbound}} + (1-p-q+a) \cdot x_{\text{bound}}}^{\text{Contribution of repressor-regulated genes}} \\ &= t \cdot x_{\text{bound}} + (1-t) \cdot x_{\text{unbound}}. \end{aligned} \tag{3}$$

As Eq. (3) shows, X simply depends on the fraction of available TF species $t = 1-p-q+2a$, where $t = T/M$, regardless of their role as activators or repressors. Importantly, global crosstalk does not directly depend on the fraction of active genes q. This is a generalization of the result obtained in [13], where the special cases of $t = q$ (all TFs are activators) and $t = 1-q$ (all TFs are repressors) were studied. To obtain a lower bound on crosstalk values for given similarity, s, and fraction of available TFs, t, we substitute the expressions for x_{bound} and x_{unbound} (Eq. (2)) into Eq. (3). We then minimize X with respect to the total TF concentration, c. Such minimization is possible because global crosstalk balances between some binding sites that should be bound and others that should be unbound. For the former, higher c increases their chance to be bound by their cognate TFs and thus reduces crosstalk. For the latter, their cognate TF is absent and thus higher c increases their chance to be bound by foreign TFs, namely increases crosstalk. We then obtain the expression for minimal crosstalk:

$$X^*(t,s) = t\left(-s(1-t) + 2\sqrt{s(1-t)}\right). \tag{4}$$

Hence, the lower bound on crosstalk X^* only depends on two macroscopic variables: s (similarity between binding sites) and t (fraction of available TFs). The higher the similarity s, the larger the resulting crosstalk X^*, where to first order, $X^* \sim \sqrt{s}$ (Fig 2A). The dependence on t is more complicated and non-monotonic: for low t values, $t < t^*(s)$ (we show in the SI that $t^*(s) \geqslant 2/3$), X^* increases with t. Intuitively, the number of available TF species positively correlates with the number of crosstalk opportunities. Contrary to this intuition, for high TF usage beyond the threshold value t^*, we find the opposite trend, where X^* *decreases* with increasing TF usage, t. This non-monotonic dependence of X^* on t comes about because the optimal concentration $c^*(s,t)$ is tailored specifically for each t value, because the relative weight of binding sites that should be bound vs. those that should be unbound, shifts with t. High TF usage though always comes at the cost of an exponential increase in the optimal TF concentration, c^*, (Eq. S4), where for high s values, c^* diverges to infinity $c^* \to \infty$ (see Fig 2B). We discuss below the biological relevance of the high t regime.

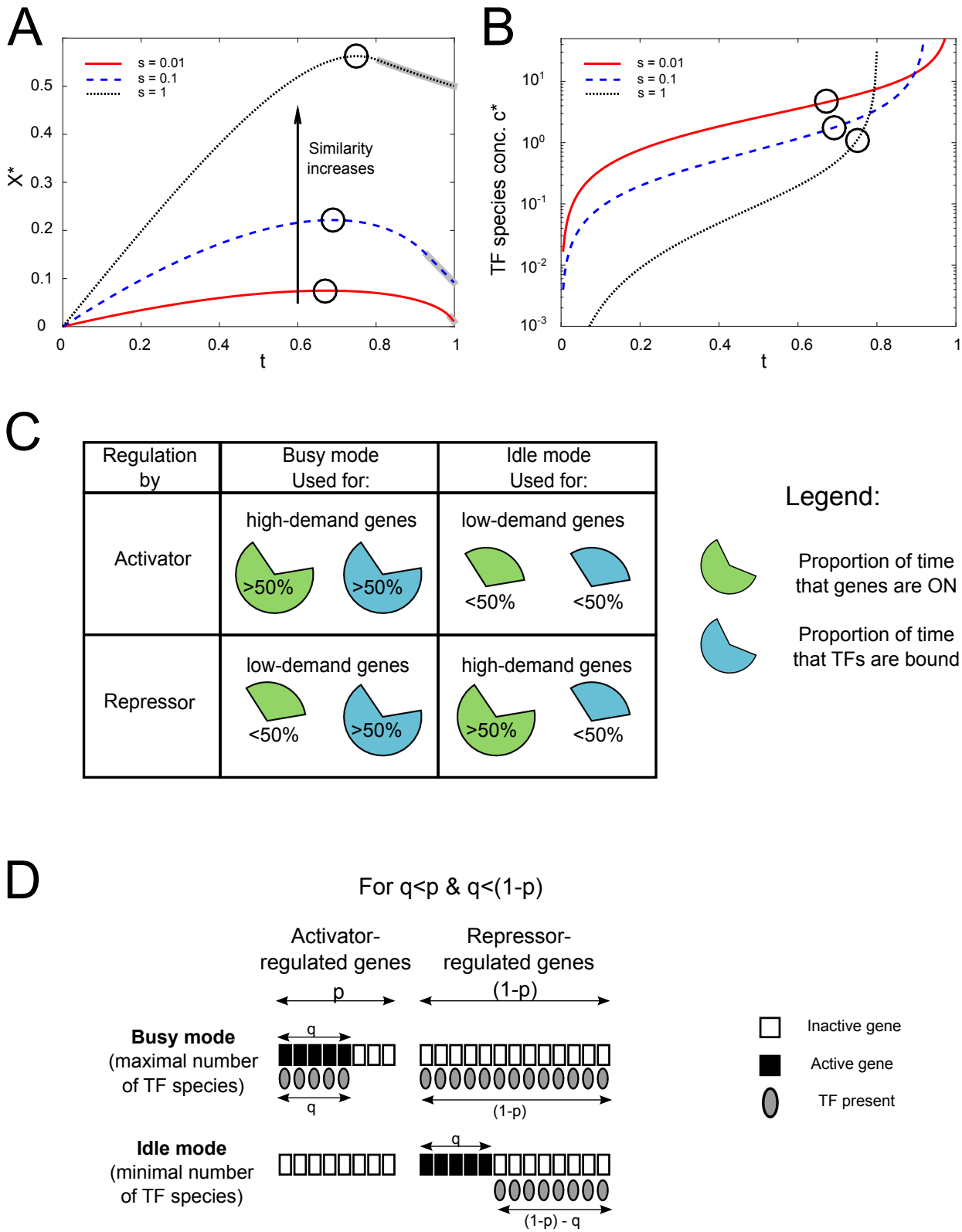

Figure 2: (Continued on the following page.)

Figure 2: **Crosstalk depends on the fraction of TFs in use, which varies between regulatory designs. (A)** We illustrate minimal crosstalk, X^*, vs. t, the fraction of TFs in use, for different values of similarity, s. In most of the parameter regime (for $t < t^*$, $t^* \geqslant 2/3$), minimal crosstalk, X^*, increases with t. Black circles denote the maxima of the curves. Crosstalk monotonically increases with similarity between binding sites. The anomalous regime where TF concentration needed to minimize crosstalk mathematically diverges to infinity, is grey-shaded around the curves. **(B)** The optimal TF concentration, c^*, needed to minimize crosstalk increases sharply with t. c^* diverges to infinity at the boundary with the anomalous regime, which for high similarity s, occurs already at lower TF usage t. Circles represent the maximal X^* values for each curve (as in (A)). **(C)** Different genes are expressed to different extents, where here, we grossly classify them as either high- (more than half of the time) or low-demand (less than half). If a high-demand gene is regulated by an activator or if a low-demand gene is regulated by a repressor, demand for the regulator will be high ('busy design'). Conversely, if the same high-demand gene is regulated by a repressor and the low-demand gene is regulated by an activator, the regulator is only required for a small fraction of the time ('idle design'). **(D)** Each of the q active genes and $1-q$ inactive genes can be assigned either positive or negative regulation. We illustrate the two extremes maximizing (minimizing) TF usage: in the 'busy' ('idle') design, as many active genes as possible are assigned positive (negative) regulation and as many inactive genes as possible are assigned negative (positive) regulation. The scheme is shown for an example with the given relationship between the proportion of active genes q, the proportion of activator-regulated p and the proportion of repressor-regulated $(1-p)$; that is, $q \leqslant p, (1-p)$. Other combinations are shown in SI Fig S5.

Mode of regulation affects global crosstalk because it affects TF usage

A particular gene activity pattern can be obtained by different combinations of positive and negative regulation, yielding seemingly identical gene functionality. One may then ask whether these various TF-gene associations differ in the resulting global crosstalk. Following Eq. (4), crosstalk only depends on the fraction of available TF species, t, regardless of the underlying association of a gene with either activator or repressor. It is thus sufficient to consider how different regulatory strategies affect TF usage, rather than analyzing the whole network architecture, thereby significantly simplifying the analysis. Using our model, we calculate the global crosstalk for any combination of the fraction of active genes, q, with any mixture of activators and repressors defined by p, thereby covering all possible gene-regulator associations with either activators or repressors. While each point represents a fixed fraction of active genes, this model can also be used to study a varying number of active genes, by taking a distribution of points over the q-axis (see SI for an example). Specifically, we focus on the two extreme gene-regulator associations, which we call the 'busy' and 'idle' network

designs. The 'busy' design means that gene regulation is operative most of the time. It is implied by the "Savageau demand rule" [2], because the gene's default state of activity is not its commonly needed state. Under the opposite 'idle' design, the default state of each gene is its more commonly needed regulatory state. Hence, regulation is inoperative most of the time (see Fig 2C). Hybrids of these two extreme designs are also possible.

To represent the 'busy' design, we associate as much of the q active proportion as possible with activators, and only if the total fraction of activators is smaller than the fraction of active genes ($p < q$), the remaining $q - p$ proportion is regulated by repressors. Thus the fraction of activator-regulated active genes is $a = \min(p, q)$. Conversely, under the 'idle' design, we associate as much of the q active proportion as possible with repressors. Only if the fraction of repressors is smaller than the proportion of active genes ($1 - p < q$), the remaining active genes pursue positive regulation, hence $a = q - \min((1 - p), q)$. The corresponding fractions of TFs in use (including both activators and repressors) in these two extremes are then:

$$t_{\text{busy}} = 1 - |p - q| \tag{5a}$$

$$t_{\text{idle}} = |1 - p - q|. \tag{5b}$$

In Fig 2D, we illustrate regulation following these two extreme designs. We show that the TF assignments defined in Eq. (5) are the two extremes in TF usage. Namely, for any general regulatory scheme, the fraction of TFs needed to regulate a given fraction of genes q is $t_{\text{idle}} \leqslant t \leqslant t_{\text{busy}}$ (see SI for formal proof).

In Fig 3A, we illustrate the difference in the fraction of available TFs between the two extreme designs $\Delta t = t_{\text{busy}} - t_{\text{idle}} = 1 - |p - q| - |1 - p - q| > 0$, demonstrating that the 'busy' design always requires more regulators than the 'idle' design (see SI).

Using Eq. (4), we obtain exact expressions for X^* under these extreme designs (see SI). In Fig 3B, we show $\Delta X^* = X^*_{\text{idle}} - X^*_{\text{busy}}$, the difference in minimal crosstalk X^* between the two extreme designs, for all (p, q) combinations. We find that the 'idle' design yields less crosstalk in a large part of this parameter space. The 'busy' design still involves less

crosstalk for parameter combinations centered around the diagonal $p = q$, whereas the 'idle' design always performs best on the anti-diagonal $1 - p = q$. This is due to the fact that on the diagonal, the fraction of activators, p, equals exactly the fraction of genes that should be active q, resulting in full usage of all existing TFs, $t = 1$. On the anti-diagonal $1 - p = q$, the fraction of genes that should be active, q, equals exactly the fraction of repressors $1 - p$. Thus, the default state of all genes is the desired regulatory state requiring no TF usage at all, $t = 0$, which makes the 'idle' design most advantageous.

In the region in which the 'busy' design yields the lowest crosstalk, this comes at the cost of using a larger fraction of existing TF species, as depicted in Fig 3C. The 'idle' design, in contrast, requires a much smaller fraction of TF species. Furthermore, the two designs differ not only in the fraction of TFs needed but also in their concentrations. To achieve the lower bound, the 'busy' design always requires a higher total TF concentration, c^* (Fig 3D).

The explanation for the alternating crosstalk advantage between the two extreme designs lies in the non-monotonic dependence of crosstalk on TF usage, t (Fig 2A). For $t(p, q) < t^*(s)$, crosstalk *increases* and for $t(p, q) > t^*(s)$, it *decreases* with t. Thus, for (p, q) combinations for which $t_{\text{idle}} < t_{\text{busy}} < t^*$, 'idle' design will yield lower crosstalk, whereas if $t^* < t_{\text{idle}} < t_{\text{busy}}$, 'busy' will be more advantageous (see SI for more details). While 'idle' and 'busy' represent the two extremes, a continuum of regulatory designs interpolating between these two extremes can be defined. We show, however, that minimal crosstalk is always obtained by one of the two extremes, due to the concavity of $X^*(t)$ (see SI).

We previously found that for some parameter combinations of similarity, s, and fraction of active genes, q, the mathematical expression for X^* (Eq. (4)) has no biological relevance [13]. Specifically, for similarity between binding sites which is too high $s > \frac{1}{1-t}$, regulation is ineffective and the lower bound on crosstalk X^* is obtained with no regulation at all. Another biologically irrelevant regime occurs for high TF usage $t > t_{\text{max}}$ (see SI of [13]). Then the concentration needed to obtain minimal crosstalk formally diverges to infinity $c^* \to \infty$. These biologically implausible regimes put an upper bound to the total number of genes that an organism can effectively regulate [26, 13]. The results shown in Fig 3 only refer to crosstalk values obtained in the 'regulation regime' where c^* is finite and

positive, $0 < c^* < \infty$. Specifically, we find that when similarity, s, increases, parts of the parameter space shown in Fig 3A indeed move into the anomalous regimes. In particular, the high TF usage region around the diagonal $p = q$, where the 'busy' design outperforms in crosstalk reduction, vanishes due to this anomaly (see Fig 3E where anomalous regions are blackened). For high similarity values $s > 5$, the 'idle' design yields lower crosstalk in the entire biologically relevant parameter space - see SI and Fig S7.

The distribution of crosstalk in a stochastic gene activity model

So far, we considered a deterministic model in which the numbers of active genes and available TF species were fixed, resulting in a single crosstalk value per (p, q) configuration. In reality, these numbers can temporally fluctuate, for example, because of the bursty nature of gene expression [27, 28]. In the deterministic model, we also assumed uniform gene usage, such that all genes are equally likely to be active. In reality, however, some genes are active more frequently than others.

To account for this, we study crosstalk in a probabilistic gene activity model. We assume independence between activities of different genes, where each gene i, $i = 1...M$, has demand (probability to be active) D_i. We then numerically calculate crosstalk for a set of genes. This approach enables us to incorporate a varying number of active genes and a non-uniform gene demand and compare our results to the deterministic model studied above. To comply with its demand D_i, each gene i is regulated with probability γ_i, where $\gamma_i = D_i$ if regulation is positive and $\gamma_i = 1 - D_i$ if it is negative. We then obtain exact solutions for the distributions of t and X^* (Eqs. S14-S14 in SI). In Fig 3F, we illustrate the X^* distributions for two values of t, representative of the two extreme designs. We find excellent agreement between this analytical solution and stochastic simulation results. The distribution of X^* is typically narrow, such that for practical purposes, the distribution mean, calculated using the deterministic activation model, serves as an excellent estimator of crosstalk values. For more details on this calculation and for approximation of the distribution width, see SI.

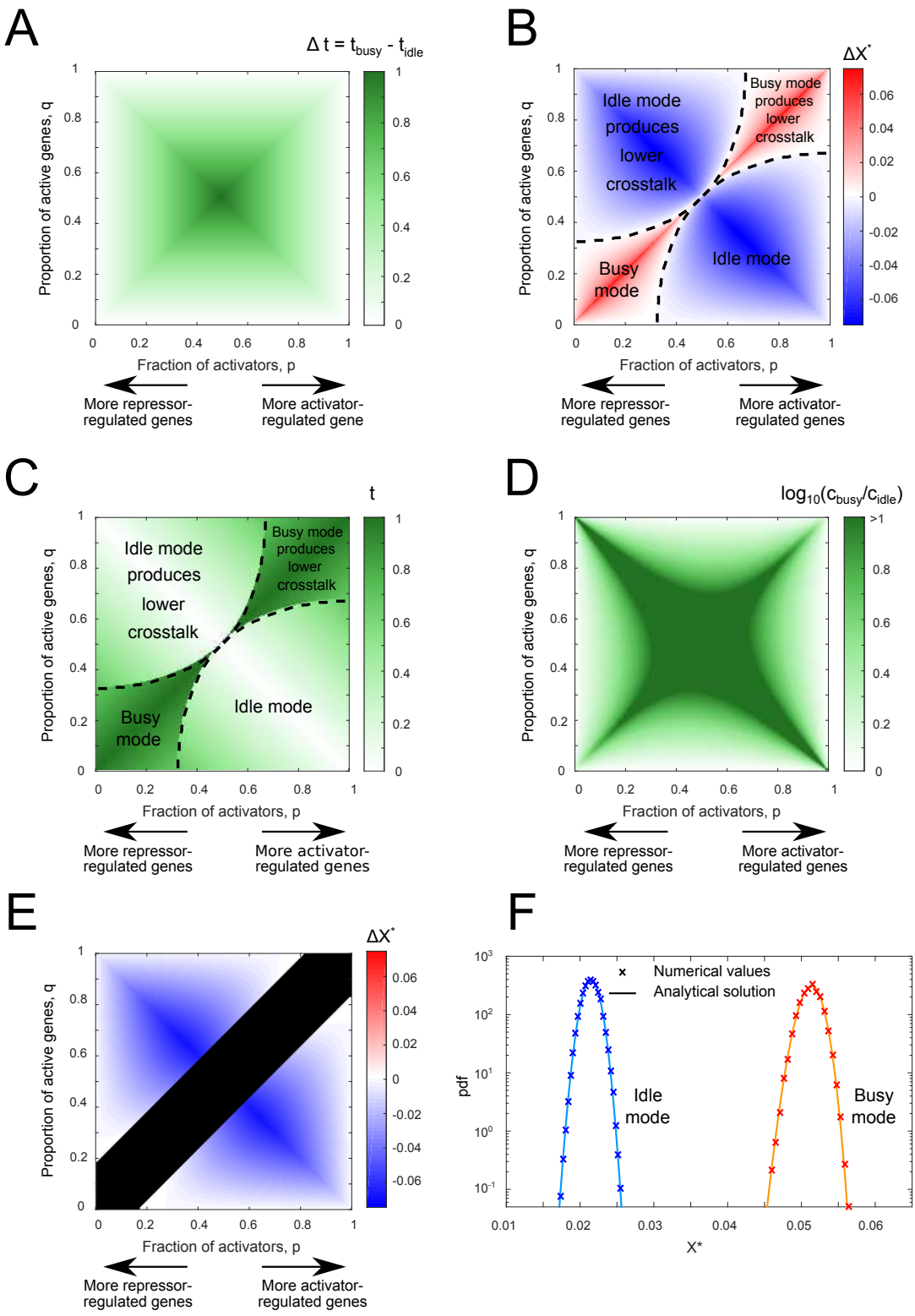

Figure 3: (Continued on the following page.)

Figure 3: **'Idle' design yields lower crosstalk than the 'busy' in a large part of the parameter regime.** **(A)** The 'busy' design always requires more TFs compared to the 'idle' design. Here we illustrate Δt (shown in color scale), i.e., the difference in the fraction of TFs in use between the two designs for different values of p and q. **(B)** The difference in total crosstalk ($\Delta X = X^*_{\text{idle}} - X^*_{\text{busy}}$) between 'idle' and 'busy' designs, shown in color scale, as a function of the fraction of activator-regulated genes p and relative number of active genes q. In a large part of the parameter regime (colored blue), lower crosstalk is achieved by following the 'idle' design. The 'busy' design is most beneficial on the diagonal $p = q$ (red region), but this requires use of all TFs and comes at the cost of an enormously high TF concentration. The 'idle' design is most beneficial around the anti-diagonal $q = 1 - p$, where regulation can proceed with no TFs at all and crosstalk is close to zero. **(C)** Fraction of TFs in use (shown in color scale) when the design providing minimal crosstalk ('idle' or 'busy' as in (b)) is used, as a function of p and q. Black dashed lines mark the borders between the regions where 'busy' or 'idle' designs provide lower crosstalk. While 'idle' design mostly requires a minority (<50%) of the TFs, the 'busy' design always necessitates a majority (>50%) of TFs to be in use. $s = 10^{-2}$ was used in (B)-(C). **(D)** Ratio between TF concentrations providing minimal crosstalk in either design $c^*_{\text{busy}}/c^*_{\text{idle}}$. 'Busy' design always requires higher TF concentrations. **(E)** For higher similarity s between binding sites, parts of the parameter space fall into the anomalous regime where the optimal TF concentration diverges to infinity. We plot here the difference in optimal crosstalk $\Delta X = X^*_{\text{idle}} - X^*_{\text{busy}}$ between designs for $s = 1$. Black areas denote the anomalous regime. Importantly, the region where the 'busy' design was beneficial for low s (see (B)) falls into this anomalous regime. **(F)** Analytical solution of the stochastic model for the distribution of crosstalk values, is in excellent agreement with stochastic simulation results. The distributions obtained are narrow, suggesting that their mean value is representative. Crosstalk values only depend on TF usage, regardless of the exact underlying model. Parameter values: total number of genes $M = 3000$, proportion of activator-regulated genes $p = \frac{1}{3}$, regulation probability $\gamma_i = \gamma = 0.12$ for 'idle' design and $\gamma_i = \gamma = 0.92$ for 'busy' design, with $2 \cdot 10^6$ realizations.

Data-based crosstalk calculation

Similarity and crosstalk, considered in our analytical model, can be estimated from bioinformatic data. As direct thorough measurements of TF binding preferences are available for only a few TFs [22, 24, 25], we use statistical estimates based on multiple binding sites to which a particular TF binds (PCM) to determine its binding energetics to various sequences. Specifically, we use data of 23 *S. cerevisiae* transcription factors collected from the scerTF database [29, 30]. PCMs are $4 \times L$ matrices that provide the total number of counts for each nucleotide at each of the L binding site positions, taken over multiple binding sites of the particular transcription factor. They allow us to compute the mismatch energy penalties for every position and nucleotide in a given binding site sequence and then numerically calculate crosstalk.

In our theoretical model, we made several simplifying assumptions to allow for an analytical solution. In particular, we assumed uniform properties for all binding sites, assigned equal energetic contributions to all nucleotides in the sequence and assumed that all TFs regulate an equal number of genes (a single gene per TF, in the basic model). The availability of TF binding data allows us to relax these assumptions, and consider variation in binding energies and promiscuity among TFs, as well as the actual unequal energetic contributions of the different positions in each binding site.

Due to shortage of data on actual concentrations, we still assume equal concentrations for all available TFs. In addition, due to paucity of data on epistatic effects between distinct binding site positions, we still assume additivity in the energetic contributions of different positions in the sequence. The latter assumption is considered reasonable for up to 3-4 bp substitutions [22].

Similarity values vary between genes even within the same organism. We begin by numerically calculating the similarity s_i between transcription factors (see Methods). In Fig 4A, we show the distribution of similarity values of genes associated with 23 *S. cerevisiae* transcription factors (top). We find a broad distribution of s_i values spanning over 5 orders of magnitude, where its median is around $10^{-4} - 10^{-3}$. This finding is in marked contrast to the full symmetry and equal s_i values for all TFs assumed in our analytical solution.

While we find that s_i values are very variable, the largest contributions to global crosstalk are made by the few most promiscuous TFs (those with high s_i values). In the following, we fit an effective similarity value that would best capture the numerically calculated crosstalk values, had all TFs had uniform s_i values, as in the mathematical model (denoted by red arrow in Fig 4A). In this example, we find that $s_{\text{effective}}$ is almost equal to the median s_i value (black arrow there).

Numerical crosstalk calculation: incorporation of a complex TF-gene interaction network. In the analytical model, we assumed that each TF regulates only a single unique gene. Yet, in real gene regulatory networks, the same TF species often regulates multiple genes and some genes are regulated by a combination of different TFs. To account for this, we expand our dataset to include all the 2126 genes [31] regulated by the 23 *S. cerevisiae* TFs for which we have PCMs and considered all possible TF-gene interactions in

this set. Notably, there is high variability in the number of genes regulated by each TF. For different values of t (proportion of available TFs), we randomly choose a subset of TFs to be available and accordingly compute the crosstalk probabilities for all genes, accounting for all possible TF-binding site (BS) combinations. We repeat this procedure for 20 different t values, with 100 independent draws of available TFs for each. In the crosstalk calculation, we assume that all available TFs have equal concentrations. In contrast to the analytical calculation, where we included crosstalk contributions from all TFs, here, only binding states associated with transcription factors that are chosen to be available, are considered.

We then fit the numerically calculated crosstalk with the analytical model, where a single $s_{\text{effective}}$ is used for all TFs. Fig 4B shows both the numerically calculated crosstalk and the analytically predicted one (using $s_{\text{effective}}$) for this more complex interaction network (solid and dashed lines, correspondingly). The grey shading represents ± 1 standard deviation around the mean value of the numerically calculated crosstalk.

Data incompleteness could affect crosstalk estimates. Global crosstalk accounts for the combined effects of all of the organism's TFs and binding sites. Unfortunately, data of TF binding preferences is incomplete. Moreover, the accuracy of PCMs depends on the number of known binding sites associated with the TF of interest. Due to these technical limitations, we focused on only 23 *S. cerevisiae* TFs for which >5 binding sites (per TF) are known. However, this small subset of TFs regulates one third (!) of the yeast genes. Motivated by that, we ask how representative is a crosstalk estimation of the entire network based on this small TF subset. In other words, what fraction of the TFs (or genes they regulate) would suffice to reliably estimate the global network crosstalk. This crosstalk estimation problem is further complicated by the diversity of s_i values we find among TFs. To generally address these questions, we simulate synthetic gene regulatory networks, each integrating 300 TFs. We simulate the binding preferences of these TFs using the PCM statistics of the 23 yeast TFs (see Methods). We then sample subnetworks of different sizes from these full networks and numerically calculate crosstalk for each subnetwork (Methods).

We sample the full networks in two manners: we either randomly choose a subset of TFs ("random subnetworks") or deterministically select the TFs showing the highest similarity with respect to the full network ("ordered subnetworks"). The latter choice is motivated by

the prior information that the few yeast TFs for which we have reliable data, are definitely not a random subset, but rather the subset that has the largest number of binding sites. Hence, we expect those TFs to be the least specific of all TFs. Alternatively, this choice can serve as a worst case estimate of global crosstalk. To compare different networks on an equal basis, we estimate the effective similarity $s_{\text{effective}}$ fitted for each subnetwork. Fig 4C shows the distributions and medians of $s_{\text{effective}}$ values obtained, as a function of the subnetwork size. Each distribution is based on independent draws of 100 full networks. From each full network, we sample one random and one ordered subnetwork of each size.

We find, that small-size "ordered" subnetworks exhibit higher median $s_{\text{effective}}$ values but narrower distributions than the "random" subnetworks, as expected. Both "ordered" and "random" subnetworks converge to the same $s_{\text{effective}}$ value for the full network (of size 300). The $s_{\text{effective}}$ distribution for the full size represents variation between various full networks of same size, which is significantly smaller than the variation due to limited sampling, observed for the smaller networks. As the "ordered" subnetworks deliberately include the most promiscuous TFs, their $s_{\text{effective}}$ is an over-estimate of the full network measure. In contrast, we find, that $s_{\text{effective}}$ estimated for random subnetworks is an under-estimate of the full network $s_{\text{effective}}$. In our synthetic data, we allowed for binding site length variation among TFs (the PCM dimension). Interestingly, we find correlation between the TF's promiscuity s_i and its consensus binding site length. An opposite effect is found for the length of DNA binding sites (see Fig. S11).

Considering the sufficiency of the sample size, for an "ordered" subnetwork, a sample of ~ 50 (out of 300) TFs provides variation close to the full network measure, whereas for "random" subnetworks, a larger sample size of around ~ 100 TFs (out of 300) is needed. Either way, we conclude that a global crosstalk estimate is possible with only a subset of the network TFs. We compare our calculated s_i values of yeast data (red cross) to the estimated $s_{\text{effective}}$ distributions of this subnetwork size. Interestingly, the yeast estimated crosstalk value falls below the median value for both "random" and "ordered" sampling approaches. This may imply that selection to reduce crosstalk is at work, yielding similarity values which are lower than what one would expect at random [32].

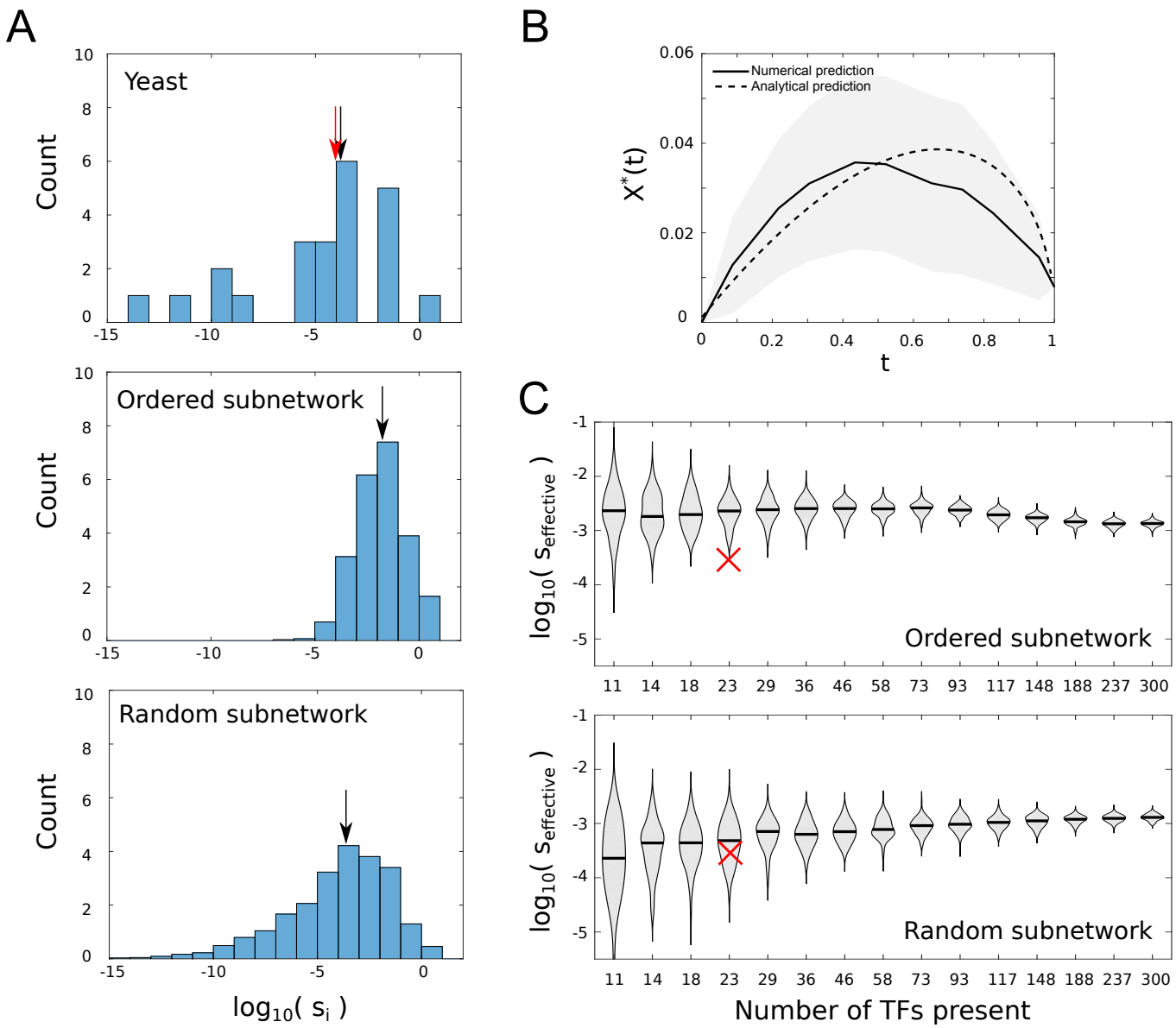

Figure 4: (Continued on the following page.)

Discussion

The existence of multiple system designs that seemingly realize the same function, is ubiquitous and often puzzling [33, 34, 35, 36]. Naturally, it raises two types of questions [2]: Are there secondary functional differences between different designs? Do such designs differ in their evolutionary accessibility (and sustainability) [37, 38] or is the existence of one or the other a mere coincidence [39, 11]? Here, we studied different gene regulatory network designs that implement the same gene activity pattern in response to a signal. We compared

Figure 4: **Data-based crosstalk estimates.** **(A)** Inter-TF similarity values of *S. cerevisiae* TFs (top), and of synthetic data (middle and bottom) exhibit broad distributions spanning a few orders of magnitude. The distribution median values are marked by black arrows. The red arrow in the yeast data represents $s_{\text{effective}}$ of the yeast data, and nearly overlaps with the distribution median. Synthetic data were created by randomly drawing PCMs representing all TFs of an artificial network. Then, sub-networks of 23 TFs were sampled by either taking the 23 most promiscuous TFs (middle) or randomly choosing them (bottom). The figures show similarity distributions amongst TFs in these artificial networks, averaged over 100 repeated draws. s_i values here are with respect to all TFs in the network, regardless of their (un)availability. **(B)** Numerical prediction of minimal global crosstalk depending on TF usage t for *S. cerevisiae* (solid line) compared to an analytical prediction based on a single $s_{\text{effective}}$ value common to all genes (dashed line). This effective similarity value was chosen to provide the best fit to the numerical curve. The curves represent estimation of crosstalk for the network of all 2126 *S. cerevisiae* downstream genes regulated by the 23 TFs, for which we have PCMs. The numerical curve represents the mean over 10^3 realizations for each t value, where the exact subset of available TFs was randomly drawn. The surrounding gray shadings show ± 1 standard deviation around the mean. The discrepancy between numerical and analytical calculations is attributed to the broad distribution of s_i values for the numerical calculation, whereas the analytical calculation assumes a uniform s_i value for all TFs. **(C)** Violin plots of $s_{\text{effective}}$ for different subnetwork sizes for *ordered* and *random* subnetworks. Ordered subnetworks are the subsets of TFs having highest similarity s_i with respect to the whole network. Random subnetworks include a random subset of the full network TFs. For each subnetwork, we numerically calculated crosstalk and fitted the $s_{\text{effective}}$ which would best capture the crosstalk function if all TFs had a uniform s value. The violin plots represent distributions of effective similarity values from 100 different randomly drawn subnetworks, each coming from an independently drawn full network of 300 TFs. The red x represents the $s_{\text{effective}}$ value of the 23 yeast TFs (same value as the red arrow in A). For details on the numerical calculations of similarities and crosstalk, see Methods. All violin plots exhibit broad $s_{\text{effective}}$ distributions which are broadest for the smallest subnetworks, as expected. For "ordered" subnetworks, the median $s_{\text{effective}}$ value is high for the small subnetworks (which were chosen to contain the most promiscuous TFs) and then slightly decreases for bigger subnetworks. For random subnetworks, the trend is opposite.

their susceptibility to transcriptional crosstalk - a typically overlooked functional aspect. We previously found a lower bound on crosstalk $X^* = X^*(t, s)$ [13], which is fully determined by two macroscopic "thermodynamic-like" variables, regardless of other microscopic details of the network. These are the fractions of available TF species, t, and the average similarity between distinct binding site sequences, s. This emergent simplification enabled us to analyze crosstalk for classes of gene regulatory networks, regardless of other network details. We found that crosstalk always increases with s. In a large part of the parameter regime, crosstalk also increased with t - the fraction of TFs that are available. We showed that different network designs may vary in the TF usage they require, and hence differ in

the crosstalk levels they incur. We analyzed two extremes: a 'busy' design, which maximizes the use of regulation and, by large, maximizes crosstalk, and the opposite 'idle' design, that minimizes the use of regulation and consequently minimizes crosstalk. We found that, the 'busy' regulatory design also requires a much higher total TF concentration. This 'busy' design is equivalent to the previously proposed Savageau demand rule [1].

We also studied a stochastic gene activation variant of the model, where the number of active genes can fluctuate. We found that it is well-approximated by the deterministic activation model, because the distributions of TF availability and minimal crosstalk are typically very narrow and centered around their mean value.

Where are real organisms located in the (t, s) parameter space? Reports of the number of co-expressed genes greatly vary between organisms and depend on growth conditions. For example: $\sim$ 10,000 different genes were reported to be co-expressed in a mouse cell ($<$50% of total) [40, 41], 10,000-12,000 ($<$50%) genes were estimated to be co-expressed in human HeLa cells [42], 3300-3500 out of 4290 genes (76%-82%) were expressed in *E. coli* during exponential growth [43, 44] and 75%-80% of the genes were expressed in *S. cerevisiae* [45, 46].

Values of similarity between distinct TF binding sites, vary not only between organisms, but also between modules and distinct genes within the same organism (see Fig 4). We estimated s_i and the resultant minimal crosstalk values for 23 *S. cerevisiae* TFs using PCM data. We found an extremely broad distribution of single-TF s_i values spanning $>$5 orders of magnitude, with a median between $10^{-4} - 10^{-3}$. Global crosstalk, however, is determined by the few high-similarity TFs. To bridge the gap between the high diversity of s_i in real networks and our uniform similarity analytical solution, we fitted a single $s_{\text{effective}}$ value which would best capture the numerically calculated network crosstalk. For the yeast data, we found that this $s_{\text{effective}}$ is very close to the distribution median. Using our estimates for s and t, we estimated minimal crosstalk X^* for this subnetwork of *S. cerevisiae* to be in the range 0.03-0.04 (see Fig 4B), if 30%-80% of the genes are co-regulated. Our analysis showed that, for relatively low s values, there was a regime in the parameter space in which 'busy' yields the lowest crosstalk, as we found for yeast. The choice of optimal network design ('busy'/'idle') depends on the proportion of co-regulated genes and the proportion

of activators. For organisms with high s values, the regime in which 'busy' is beneficial is actually anomalous, and hence biologically irrelevant. Such higher s is expected for organisms with shorter binding sites.

Binding site data is often incomplete. To assess the validity of whole-network crosstalk estimation based on a small subset of TFs, we constructed synthetic gene regulatory networks, sampled some subnetworks and then compared the s estimation of full and partial networks. In the *S. cerevisiae* case, we found that a full network crosstalk estimate is possible with binding information of only 16%-33% of the TFs.

Our analysis determined a lower bound for crosstalk. Some of our simplifying assumptions were lenient and crosstalk may be higher than predicted by our model. For example, we assumed that total TF concentration is accurately tuned. In reality, TFs are not necessarily expressed and degraded at a precise time [47]. Other simplifications that may have affected crosstalk estimates include the averaging over gene sets of same-size as representatives of different environmental conditions, whereas, in reality, the number of expressed genes could vary between environments (e.g., growth media [43]). We averaged over all possible choices of active genes, although only some of these activity combinations occur naturally. We also assumed that every gene has a regulator, and vice versa, although this is not always the case. Hershberg and co-workers found an imbalance between genes and regulators, where orphan repressors with no genes and orphan genes with no activators, transiently exist, and could also contribute to crosstalk [48].

Our study demonstrated the pervasive impact of a new type of protein production cost which is typically overlooked: that of regulatory interference caused by excess proteins in the dense cellular medium. This regulatory cost is distinct from the energetic burden of unnecessary protein production, which was found to delay growth [8, 9, 10, 49]. The regulatory cost increases super-linearly with the number of molecular species and regulatory interactions. Hence, it is exposed only when the network is considered as a whole.

It was previously shown that transcriptional error for a single gene is minimized when its binding site is occupied [6]. However, single-gene studies failed to consider the potential interaction of the regulators occupying the binding sites with other genes, causing extra crosstalk. This additional regulatory cost could also play an evolutionary role and bias

the choice between otherwise equivalent network designs. Selection to reduce regulatory crosstalk [50, 32], or 'negative design' in protein-protein interactions [51, 52], has been proposed by previous studies. Our finding that similarity between *S. cerevisiae* TFs is lower than what would be obtained in a random network with similar parameters, corroborated these reports. Theoretical [33, 53] and experimental [54, 38, 55] works highlighted the role of crosstalk in gene regulation and signaling as promoting network evolvability. However, the interplay between the opposing effects of crosstalk, i.e., impaired signaling reliability on short time scales, alongside promotion of network evolvability in the long run, is not fully understood. Taken together, a generalized model for network evolution, which would incorporate the effects of crosstalk on different time scales, alongside traditional selection on the network to achieve a certain input-output goal, remains to be formulated.

Methods

Distribution of t is approximated by a Gaussian distribution. Given that a gene i has its cognate TF present with a probability γ_i ($i \in (1, M)$, where M is the total number of genes), the distribution of available transcription factor species in the system follows Poisson-binomial distribution. This is the probability distribution of a sum of independent Bernoulli trials that are not necessarily identically distributed, each with probability γ_i. Its mean and variance are:

$$\langle t \rangle = \frac{1}{M} \sum_{i=1}^{M} \gamma_i = \langle \gamma_i \rangle, \tag{6}$$

$$\mathrm{var}(t) = \frac{1}{M} \sum_{i=1}^{M} \gamma_i (1 - \gamma_i) = \langle \gamma_i (1 - \gamma_i) \rangle. \tag{7}$$

As this distribution is difficult to compute for large values of M, we can follow the central limit theorem and approximate it by a Gaussian distribution with the same mean and variance.

Exact solution of probability distribution of X^*. For a function $X^*(t)$, where t is a random variable with probability distribution $f_t(t)$, the probability distribution of X^*, $f_{X^*}(X^*)$ is:

$$f_{X^*}(X^*) = \sum_i f_t(g_i^{-1}(X^*)) \left| \frac{\mathrm{d}g_i^{-1}(X^*)}{\mathrm{d}X^*} \right|, \tag{8}$$

where $g_i^{-1}(X^*) = t_i$ represents the inverse function of the $i-$th branch. In our case with two branches:

$$f_{X^*}(X^*) = f_t(g_1^{-1}(X^*)) \left| \frac{\mathrm{d}g_1^{-1}(X^*)}{\mathrm{d}X^*} \right| + f_t(g_2^{-1}(X^*)) \left| \frac{\mathrm{d}g_2^{-1}(X^*)}{\mathrm{d}X^*} \right|. \tag{9}$$

The solutions for $g_i^{-1}(X^*)$ and its derivative exist for crosstalk $X^*(t)$ and can be analytically computed. Therefore, the solution for the distribution of minimal crosstalk $f_{X^*}(X^*)$ is also analytically known.

For regime I, the lower limit on crosstalk is $X^*(t) = t$. Its inverse is $g^{-1}(X^*) = t(X^*) = X^*$,

while the derivate $\mathrm{d}g^{-1}(X^*)/\mathrm{d}X^* = 1$. Similarly, in regime II, the lower limit of crosstalk equals $X^*(t) = 1-t/(1+\alpha t)$, the inverse function $g^{-1}(X^*) = t(X^*) = (1-X^*)/(1-\alpha+\alpha X^*)$, and its derivate $\mathrm{d}g^{-1}(X^*)/\mathrm{d}X^* = -(1-\alpha-\alpha X^*)^{-2}$. The analytical solution for regime III was computed using Mathematica and the solution can be found in SI.

Using these values, one can compute $f_{X^*}(X^*)$ for X^* coming from any of the three regimes.

Stochastic semi-analytical solution of crosstalk for a random number of TFs present. For each gene i, we randomly draw, with probability γ_i, that its cognate TF is available. We then obtain the proportion t of available TFs. As this process is stochastic, the proportion t differs between different realizations. Next, we compute the lower limit on crosstalk $X^*(t)$ for this t value using the analytical solution. The crosstalk is computed in regime I, II or III, as needed. Using multiple realizations ($=10^6$) of t, we numerically obtain the distribution of crosstalk values for values of $t \in (0, 1)$.

Obtaining the energy matrices from position count matrices (PCMs). Position count matrices (PCMs) document the binding site sequences of TFs. Each element c_{ij} designates the number of known TF binding site sequences with nucleotide i in position j. We obtained the PCMs from the scerTF database for *S. cerevisiae*. Given these, we calculated the energy matrices which are needed to compute the similarity measure, in the following way: for a position j and nucleotide $i \in \{A, C, G, T\}$, we computed the energy mismatch value as $\epsilon_{ij} = \log\left(\frac{c_{mj}}{c_{ij}}\right)$, where c_{ij} is the count of nucleotide i in position j and $c_{mj} = \max_i c_{ij}$ is the nucleotide at the position j with the maximal count. In case of zero counts, $c_{ij} = 0$, where the energy ϵ_{ij} diverges, we added a constant pseudocount $\delta = 0.1$ to matrix entries.

Some technicalities and concerns regarding PCM usage When computing the energy matrices using PCMs, certain issues arise that could strongly bias the results if not properly addressed;

- *Inequality of total counts between positions* in PCM data. The sum of counts over all 4 nucleotides in a given PCM should be equal for all positions, but occasionally,

positions with different total counts are found. As they bias our occurrence statistics (and hence our energy calculation), we used only PCMs in which the total count was equal throughout.

- *Zero counts* in the PCMs. Many PCMs include zero counts for certain nucleotides at specific positions, rendering that element of the energy matrix undefined. Here, we applied a commonly used practice of adding a pseudocount δ to all PCM entries. Following a previous work [13], where various δ values were compared to an information method (where pseudocount is not needed), we took $\delta = 0.1$.

- *Count number sufficiency.* To achieve a reliable estimation of energies in the energy matrix, we only used PCMs with at least $p_{\text{counts}} = 5$ counts per position.

In total, we found 196 TF PCMs, but due to the above concerns, we considered only 23 of them in our calculations.

Numerical computation of similarity measure using PCMs. To compute the similarity measure between binding site k and a transcription factor l, we first substituted the sequence of BS k by the *consensus* sequence of its cognate TF k. The consensus sequence is obtained by taking the most common nucleotide in each position j. As the given binding site and TF consensus sequence are not necessarily of the same length, we distinguished between the following cases:

- If the TF consensus sequence l was shorter than the binding site sequence k, we computed the energies for all possible overlaps of the shorter sequence with respect to the longer one. We took the minimal value to be the binding energy.

- If the TF consensus sequence l was longer than the binding site sequence k, the TF energy matrix was again slid over the binding site and energies were calculated again for every relative positioning of the two sequences. The only difference from the previous case was that energetic contributions from positions where the TF binds outside the binding site, were taken into account by averaging energies over all four nucleotides. In other words, total binding energy $E = E_1 + E_2$ is the sum of contributions from

nucleotides inside (E_1) and outside (E_2) the binding site. The energy contribution of positions j outside of BS equals $E_2 = \sum_j E_{2j}$, with $E_{2j} = \sum_{i=1}^{4} \epsilon_{ij}/4$ being the average binding energy at position j (ϵ_{ij} represent elements in the energy matrix). Here too, we computed the binding energy for all possible overlaps between the BS and TF. Then, the lowest energy was taken as the binding energy E_{kl}.

This provides the matrix of binding energies E^{kl} between every binding site k and every TF l. Importantly, this binding energy is asymmetric, namely $E^{kl} \neq E^{lk}$. Hence, the similarity measure between binding site k and all other binding sites was computed as:

$$S_k = \frac{1}{T} \sum_{l=1,\ l\neq k}^{M} C_l e^{-E^{kl}}, \tag{10}$$

with C_l being the concentration of TF species l, and T the number of present TF species. In other words, the similarity S_k is the average Boltzmann weight, taken over all non-cognate TF binding to binding site k.

Numerical computation of crosstalk given PCMs. For the numerical computation of crosstalk, we used the matrix of binding energies E^{kl} between binding site k and TF l, as per the following protocol:

1. randomly choose a subset t (e.g., $t = 0.2$ represents a fifth of all TFs) of all TFs that should be regulated by their cognate TF. With each realization, a different subset is chosen.

2. For gene k, obtain the similarity measure $S_k = \frac{1}{T}\sum_{l\neq k} C_l e^{-E^{kl}}$, with C_l being the concentration of TF l, and T the number of present TF species. The concentration of absent TFs is zero. We assume that all TFs have same concentration ($C_l = C$), as in the analytical calculation.

3. Compute the probabilities that a crosstalk state occurs at any given gene, using the thermodynamic model. Other parameters include the energy difference between unbound and cognate state E_a which does not affect the final crosstalk result, and the concentration of the transcription factors, C.

4. Compute probability of crosstalk state occurrence for every gene and then obtain the total crosstalk X by summing all the individual contributions of the genes.

5. Average over a large number of realizations (we used several hundred realizations for which the average crosstalk had already converged).

6. Repeat this procedure (each with multiple realizations) using a different concentration value C each time. Then, pick the one that yields the lowest crosstalk value to be $X^*(t)$.

Numerical computation of crosstalk where each TF regulates multiple genes. In an actual gene regulatory network, many TFs regulate multiple genes and many genes are regulated by multiple TFs rather than the one-to-one TF-gene association we considered so far. Specifically, in our data, around 96% of the TFs regulate more than one gene. To account for that, we obtained the list of genes that are regulated by the given *S. cerevisiae* transcription factors [31].

This computation closely followed the previous procedure. The main difference was in the computation of the similarity measure of genes regulated by multiple cognate TFs. We now have multiple binding site sequences per gene (one for each cognate TF) and, as a result, more binding energies and similarity measures. To take this into account, for each gene, we averaged the similarity measures over its different binding sequences, as per the following protocol:

1. For a given gene k, find all the TFs that regulate it.

2. Obtain the consensus sequences of these TFs.

3. Assume each such consensus sequence represents a potential binding site sequence of gene k (same as in the case of only one TF regulating each gene).

4. Compute the similarity measure S_{k^i} between each potential binding site sequence i of gene k and all other TFs; this is done in the same way as for one TF regulating one gene using Eq. 10.

5. Use the mean of the computed S_{k^i} similarity measures taken over the various binding sites of gene k as the effective similarity of that gene.

The rest of the procedure followed the previous calculation, where each TF had only one cognate binding site: i) use the new similarity measure and compute the probability of crosstalk states, ii) do this for all genes, iii) compute the total crosstalk, iv) average over different random choices of the set of t genes, and v) minimize X with respect to the concentration C to obtain the $X^*(t)$.

Simulating synthetic data To simulate synthetic data of TF binding preferences, we constructed artificial PCMs, using the statistics of the 23 yeast energy matrices, as follows. We first created the nucleotide distribution of the yeast TFs consensus sequence and then drew random realizations from this distribution to obtain a consensus sequence of each new TF. This distribution was non-uniform and was biased towards excess of A and T nucleotides. In doing so, we allowed for an unequal length of consensus sequences, as in the yeast data (using the same length distribution). We then created the distribution of the non-consensus energy values of the 23 TFs energy matrices. To construct synthetic energy matrices for these "TFs", we drew random realizations from this distribution.

Computing the subnetworks of synthetic data and their crosstalk To construct a full network, we fabricated data for 300 TFs, computing the energy matrix and consensus sequence for each. We next computed the network's matrix of binding energies $E^{kl}_{\text{full network}}$ of the l-th TF to the k-th binding site, following the same procedure as for yeast data. We next formed subnetworks of this full network, by choosing a subset of TFs and taking the corresponding subset of binding energy entries, to obtain $E^{kl}_{\text{subnetwork}}$. We used either randomly chosen subsets of TFs ("random networks") or deterministically picked the subset of TFs having the highest similarity measure $S_i^{\text{full network}}$ with respect to the full network. We repeated this procedure for 100 randomly drawn full networks.

We then numerically computed minimal crosstalk X^* for each subnetwork, following the same procedure as for yeast data.

Comparison of numerical results to analytical expression We fit the analytical expression for $X^*(t)$ to the numerically calculated crosstalk. The main difference between the two approaches is that the analytical expression assumes uniform s values for all TFs, whereas the numerical approach allows for diverse s values. We assumed a single representative $s_{\text{effective}}$ value that would best fit the numerical result. For this, we minimized the sum of squared differences over various values of t to find the best $s_{\text{effective}}$. Distributions of $s_{\text{effective}}$ values were based on 100 randomly drawn full networks from which subnetworks were sampled. For each subnetwork size, we sampled each of the full networks just once, to avoid correlations between the random subnetworks.

Acknowledgements We thank U. Alon and Y. Pilpel for raising the question that triggered this study. We thank Nick Barton, Yonatan Friedman, Avi Mayo, Tiago Paixão, Gašper Tkačik and Marcin Zagorski for comments on the manuscript.

References

[1] Michael A. Savageau. Genetic Regulatory Mechanisms and the Ecological Niche of Escherichia coli. *Proceedings of the National Academy of Sciences*, 71(6):2453–2455, June 1974.

[2] M. A. Savageau. Design of molecular control mechanisms and the demand for gene expression. *Proceedings of the National Academy of Sciences*, 74(12):5647–5651, December 1977.

[3] M. A. Savageau. Regulation of differentiated cell-specific functions. *Proceedings of the National Academy of Sciences*, 80(5):1411–1415, March 1983.

[4] Ulrich Gerland and Terence Hwa. Evolutionary selection between alternative modes of gene regulation. *Proceedings of the National Academy of Sciences*, 106(22):8841–8846, June 2009.

[5] Michael A. Savageau. Demand Theory of Gene Regulation. I. Quantitative Development of the Theory. *Genetics*, 149(4):1665–1676, August 1998.

[6] Guy Shinar, Erez Dekel, Tsvi Tlusty, and Uri Alon. Rules for biological regulation based on error minimization. *Proceedings of the National Academy of Sciences of the United States of America*, 103(11):3999–4004, March 2006.

[7] Vered Sasson, Irit Shachrai, Anat Bren, Erez Dekel, and Uri Alon. Mode of Regulation and the Insulation of Bacterial Gene Expression. *Molecular Cell*, 46(4):399–407, May 2012.

[8] Arthur L. Koch. The protein burden oflac operon products. *Journal of Molecular Evolution*, 19(6):455–462, November 1983.

[9] C. G. Kurland and Henjiang Dong. Bacterial growth inhibition by overproduction of protein. *Molecular Microbiology*, 21(1):1–4, July 1996.

[10] Erez Dekel and Uri Alon. Optimality and evolutionary tuning of the expression level of a protein. *Nature*, 436(7050):588–592, July 2005.

[11] Mahendra Kumar Prajapat, Kirti Jain, Debika Choudhury, Nikhil Raj, and Supreet Saini. Revisiting demand rules for gene regulation. *Molecular BioSystems*, 12(2):421–430, 2016.

[12] Sarah A. Cepeda-Humerez, Georg Rieckh, and Gašper Tkačik. Stochastic Proofreading Mechanism Alleviates Crosstalk in Transcriptional Regulation. *Physical Review Letters*, 115(24):248101, December 2015.

[13] Tamar Friedlander, Roshan Prizak, Călin C. Guet, Nicholas H. Barton, and Gašper Tkačik. Intrinsic limits to gene regulation by global crosstalk. *Nature Communications*, 7:12307, August 2016.

[14] Madeline A. Shea and Gary K. Ackers. The OR control system of bacteriophage lambda: A physical-chemical model for gene regulation. *Journal of Molecular Biology*, 181(2):211–230, January 1985.

[15] P. H. Von Hippel and O. G. Berg. On the specificity of DNA-protein interactions. *Proceedings of the National Academy of Sciences*, 83(6):1608, 1986.

[16] Ulrich Gerland, J. David Moroz, and Terence Hwa. Physical constraints and functional characteristics of transcription factor–DNA interaction. *Proceedings of the National Academy of Sciences*, 99(19):12015–12020, 2002.

[17] Lacramioara Bintu, Nicolas E Buchler, Hernan G Garcia, Ulrich Gerland, Terence Hwa, Jané Kondev, and Rob Phillips. Transcriptional regulation by the numbers: models. *Current Opinion in Genetics & Development*, 15(2):116–124, April 2005.

[18] Justin B. Kinney, Anand Murugan, Curtis G. Callan, and Edward C. Cox. Using deep sequencing to characterize the biophysical mechanism of a transcriptional regulatory

sequence. *Proceedings of the National Academy of Sciences*, 107(20):9158–9163, May 2010.

[19] Michael Lässig. From biophysics to evolutionary genetics: statistical aspects of gene regulation. *BMC Bioinformatics*, 8(6):1–21, 2007.

[20] Allan Haldane, Michael Manhart, and Alexandre V. Morozov. Biophysical Fitness Landscapes for Transcription Factor Binding Sites. *PLOS Computational Biology*, 10(7):e1003683, July 2014.

[21] A. Sarai and Y. Takeda. Lambda repressor recognizes the approximately 2-fold symmetric half-operator sequences asymmetrically. *Proceedings of the National Academy of Sciences*, 86(17):6513–6517, September 1989.

[22] Sebastian J. Maerkl and Stephen R. Quake. A Systems Approach to Measuring the Binding Energy Landscapes of Transcription Factors. *Science*, 315(5809):233–237, January 2007.

[23] Zeba Wunderlich and Leonid A. Mirny. Different gene regulation strategies revealed by analysis of binding motifs. *Trends in Genetics*, 25(10):434–440, October 2009.

[24] Polly M. Fordyce, Doron Gerber, Danh Tran, Jiashun Zheng, Hao Li, Joseph L. DeRisi, and Stephen R. Quake. *De novo* identification and biophysical characterization of transcription-factor binding sites with microfluidic affinity analysis. *Nature Biotechnology*, 28(9):970–975, September 2010.

[25] Ariel Afek, Joshua L. Schipper, John Horton, Raluca Gordân, and David B. Lukatsky. Protein-DNA binding in the absence of specific base-pair recognition. *Proceedings of the National Academy of Sciences*, page 201410569, October 2014.

[26] Shalev Itzkovitz, Tsvi Tlusty, and Uri Alon. Coding limits on the number of transcription factors. *BMC Genomics*, 7(1):239, September 2006.

[27] Ido Golding, Johan Paulsson, Scott M. Zawilski, and Edward C. Cox. Real-Time Kinetics of Gene Activity in Individual Bacteria. *Cell*, 123(6):1025–1036, December 2005.

[28] Yufang Wang, Ling Guo, Ido Golding, Edward C. Cox, and N. P. Ong. Quantitative Transcription Factor Binding Kinetics at the Single-Molecule Level. *Biophysical Journal*, 96(2):609–620, January 2009.

[29] Audrey P. Gasch, Paul T. Spellman, Camilla M. Kao, Orna Carmel-Harel, Michael B. Eisen, Gisela Storz, David Botstein, and Patrick O. Brown. Genomic Expression Programs in the Response of Yeast Cells to Environmental Changes. *Molecular Biology of the Cell*, 11(12):4241–4257, December 2000.

[30] Aaron T. Spivak and Gary D. Stormo. ScerTF: a comprehensive database of benchmarked position weight matrices for Saccharomyces species. *Nucleic Acids Research*, 40(D1):D162–D168, January 2012.

[31] Saccharomyces Genome Database | SGD.

[32] Long Qian and Edo Kussell. Genome-Wide Motif Statistics are Shaped by DNA Binding Proteins over Evolutionary Time Scales. *Physical Review X*, 6(4):041009, October 2016.

[33] Tamar Friedlander, Roshan Prizak, Nicholas H. Barton, and Gašper Tkačik. Evolution of new regulatory functions on biophysically realistic fitness landscapes. *Nature Communications*, 8(1):216, August 2017.

[34] Tsvi Tlusty, Albert Libchaber, and Jean-Pierre Eckmann. Physical Model of the Genotype-to-Phenotype Map of Proteins. *Physical Review X*, 7(2):021037, June 2017.

[35] A. Wagner. Robustness and evolvability: a paradox resolved. *Proceedings of the Royal Society B: Biological Sciences*, 275(1630):91–100, 2008.

[36] O. C. Martin, A. Krzywicki, and M. Zagorski. Drivers of structural features in gene regulatory networks: From biophysical constraints to biological function. *Physics of Life Reviews*, 17:124–158, July 2016.

[37] Tamar Friedlander, Avraham E. Mayo, Tsvi Tlusty, and Uri Alon. Mutation Rules and the Evolution of Sparseness and Modularity in Biological Systems. *PLoS ONE*, 8(8), August 2013.

[38] Joshua L. Payne and Andreas Wagner. The Robustness and Evolvability of Transcription Factor Binding Sites. *Science*, 343(6173):875–877, February 2014.

[39] W. Fontana and L. W. Buss. What would be conserved if "the tape were played twice"? *Proceedings of the National Academy of Sciences*, 91(2):757–761, January 1994.

[40] Mark G. Carter, Alexei A. Sharov, Vincent VanBuren, Dawood B. Dudekula, Condie E. Carmack, Charlie Nelson, and Minoru SH Ko. Transcript copy number estimation using a mouse whole-genome oligonucleotide microarray. *Genome Biology*, 6:R61, June 2005.

[41] Saiful Islam, Amit Zeisel, Simon Joost, Gioele La Manno, Pawel Zajac, Maria Kasper, Peter Lönnerberg, and Sten Linnarsson. Quantitative single-cell RNA-seq with unique molecular identifiers. *Nature Methods*, 11(2):163–166, February 2014.

[42] Nagarjuna Nagaraj, Jacek R. Wisniewski, Tamar Geiger, Juergen Cox, Martin Kircher, Janet Kelso, Svante Pääbo, and Matthias Mann. Deep proteome and transcriptome mapping of a human cancer cell line. *Molecular Systems Biology*, 7(1):548, January 2011.

[43] Han Tao, Christoph Bausch, Craig Richmond, Frederick R. Blattner, and Tyrrell Conway. Functional Genomics: Expression Analysis ofEscherichia coli Growing on Minimal and Rich Media. *Journal of Bacteriology*, 181(20):6425–6440, October 1999.

[44] Yan Wei, Jian-Ming Lee, Craig Richmond, Frederick R. Blattner, J. Antoni Rafalski, and Robert A. LaRossa. High-Density Microarray-Mediated Gene Expression Profiling of Escherichia coli. *Journal of Bacteriology*, 183(2):545–556, January 2001.

[45] Sina Ghaemmaghami, Won-Ki Huh, Kiowa Bower, Russell W. Howson, and others. Global analysis of protein expression in yeast. *Nature*, 425(6959):737, 2003.

[46] *Genes IX 9th edition by Lewin, Benjamin published by Jones & Bartlett Publishers Hardcover*. Jones & Bartlett Publishers, March 2007.

[47] Morgan N. Price, Adam M. Deutschbauer, Jeffrey M. Skerker, Kelly M. Wetmore, Troy Ruths, Jordan S. Mar, Jennifer V. Kuehl, Wenjun Shao, and Adam P. Arkin. Indirect

and suboptimal control of gene expression is widespread in bacteria. *Molecular Systems Biology*, 9(1):660, January 2013.

[48] Ruth Hershberg and Hanah Margalit. Co-evolution of transcription factors and their targets depends on mode of regulation. *Genome Biology*, 7:R62, 2006.

[49] Irit Shachrai, Alon Zaslaver, Uri Alon, and Erez Dekel. Cost of Unneeded Proteins in E. coli Is Reduced after Several Generations in Exponential Growth. *Molecular Cell*, 38(5):758–767, June 2010.

[50] Matthew W. Hahn, Jason E. Stajich, and Gregory A. Wray. The Effects of Selection Against Spurious Transcription Factor Binding Sites. *Molecular Biology and Evolution*, 20(6):901–906, June 2003.

[51] Ali Zarrinpar, Sang-Hyun Park, and Wendell A. Lim. Optimization of specificity in a cellular protein interaction network by negative selection. *Nature*, 426(6967):676–680, December 2003.

[52] Jingshan Zhang, Sergei Maslov, and Eugene I. Shakhnovich. Constraints imposed by non-functional protein–protein interactions on gene expression and proteome size. *Molecular Systems Biology*, 4(1):210, January 2008.

[53] Michael A. Rowland, Joseph M. Greenbaum, and Eric J. Deeds. Crosstalk and the evolvability of intracellular communication. *Nature Communications*, 8:ncomms16009, July 2017.

[54] Ryan K. Shultzaberger, Sebastian J. Maerkl, Jack F. Kirsch, and Michael B. Eisen. Probing the Informational and regulatory plasticity of a transcription factor DNA–binding domain. *PLoS genetics*, 8(3), 2012.

[55] Christopher D. Aakre, Julien Herrou, Tuyen N. Phung, Barrett S. Perchuk, Sean Crosson, and Michael T. Laub. Evolving New Protein-Protein Interaction Specificity through Promiscuous Intermediates. *Cell*, 163(3):594–606, October 2015.